



Yang, X., Shah, S. A., Ren, A., Fan, D., Zhao, N., Zheng, S., Wang, W., Soh, P. J. and Abbasi, Q. H. (2018) S-band sensing-based motion assessment framework for cerebellar dysfunction patients. *IEEE Sensors Journal*, (doi:[10.1109/JSEN.2018.2861906](https://doi.org/10.1109/JSEN.2018.2861906))

This is the author's final accepted version.

There may be differences between this version and the published version. You are advised to consult the publisher's version if you wish to cite from it.

<http://eprints.gla.ac.uk/166048/>

Deposited on: 01 August 2018

Enlighten – Research publications by members of the University of Glasgow  
<http://eprints.gla.ac.uk>

# S-Band Sensing-Based Motion Assessment Framework for Cerebellar Dysfunction Patients

Xiaodong Yang, *Senior Member, IEEE*, Syed Aziz Shah, Aifeng Ren, Dou Fan, Nan Zhao, Shufeng Zheng, Wei Zhao, Weigang Wang, Ping Jack Soh, *Senior Member, IEEE*, Qammer H. Abbasi, *Senior Member IEEE*

**Abstract** — Cerebellar dysfunction (CD) is a neurological disorder that involves a number of abnormalities that affect the movement of various parts of the body such as gait abnormality or tremors in limbs such as hands or feet while reaching out for something. A user-friendly tool that can objectively evaluate the aforementioned body movements in CD patients can aid the clinicians for an objective assessment in clinical settings. The objective of this work is to develop a method that quantifies the gait abnormality and tremors in hand using S-Band sensing technique. The S-Band sensing essentially leverages small wireless devices such as network interface card, omnidirectional antenna and router operating at 2.4 GHz to record the wireless channel data. Specifically, the aim is to use the variances of amplitude and phase information induced due to the human body movements. Each body movement leaves a unique imprint in the form of wireless channel information that is used to identify abnormalities in body motions. The proposed framework applied a linear transformation on raw phase data for calibrations since the data retrieved using interface card contain noise and is inapplicable for motion detection. The support vector machine used to classify the data achieved high classification accuracy.

**Index Terms** — S-Band Sensing, Disease Detection, Motion Disorder

## I. INTRODUCTION

The cerebellar syndromes involve a number of abnormalities associated with limb movements and coordination of different parts of the body [1]. The two main types of these abnormalities

The paper is submitted on

The work was supported in part by the National Natural Science Foundation of China (Grant No. 61671349 and 61301175), in part by the China Postdoctoral Science Foundation funded project (Grant No. 2018T111023), in part by the International Scientific and Technological Cooperation and Exchange Projects in Shaanxi Province (Grant No. 2017KW-005), in part by the Fundamental Research Funds for the Central Universities (Grant No. JB180205).

Xiaodong Yang, Aifeng Ren, Dou Fan, Nan Zhao, Shufeng Zheng are with School of Electronic Engineering, Xidian University, Xi'an, Shaanxi, 710071, China.

Syed Aziz Shah is with the School of International Education, Xidian University, Xi'an, Shaanxi, 710071, China.

Wei Zhao is with the School of Electro-Mechanical Engineering, Xidian University, Xi'an, Shaanxi, 710071, China.

Weigang Wang is with Northwest Women's and Children's Hospital, Xi'an, Shaanxi, 710061, China.

Ping Jack Soh is with the Adv. Communication Engineering (ACE) CoE, School of Computer and Communication Engineering, Universiti Malaysia Perlis, 02600 Arau, Perlis, MALAYSIA

Qammer H. Abbasi is with the School of Engineering, University of Glasgow, G12 8QQ, UK.

include walking or gait abnormality, generally known as ataxia, where a CD patient stagger around and is very unsteady when walking, with poor balance. There can be other parts of the nervous system that is responsible for an in-coordinated walk, but the middle part is the common place of dysfunction. The second type of in-coordination in cerebellar dysfunction is the limb movements. For example, a CD patient trying to reach out and grab something with the hand could result in inaccurate movement, or the same thing goes with the leg, if this patient is trying to reach out using a foot. This kind of dysfunction usually comes from the side of the cerebellum. In general, gait abnormality and hand tremors are two main indicators to detect cerebellar dysfunction disorders.

Various research methods have been used to detect gait abnormality and tremors, which can be roughly classified into three categories: radar based approaches, sensor based approaches and camera based approaches. Radar based approaches used predefined features from the time-frequency representation (TFR) of the radar return signal to monitor human gait [2]. Sensor based approaches detect gait abnormality or tremors using contact sensors such as MetaMotionR – an Inertial Measurement Unit (IMU) sensor from Mbientlab [3] and the Axivity AX3 accelerometer [4]. Camera based approaches recognizes gait abnormality or tremors using the Kinect camera [5], [6].

In this paper, a framework leveraging access point and a network interface that estimates these two primary indicators - gait abnormality and hand tremors - is presented for detecting cerebellar dysfunction disorders. Compared with the above methods, the method is non-invasive, thus not requiring any device deployment on subject's body, can be implemented on commodity devices, protects the patient's privacy and presents fine-grained motion detection. The key idea is to leverage the disturbances occurred in the wireless medium due to human body's motion when the host computer is connected to the access point using network interface card (NIC). Some studies have extracted sleep-specific subject-invariant features and captured the temporal progression of sleep from RF signals [7]. The technique can also be used to detect person's respiratory behavior.

The main contributions of the proposed study are:

- 1) **Characterization of CD Motion:** Firstly, we present that the channel information retrieved from the host computer reflects the fine-grained human motions. The experiments are performed on small wireless devices to record the wireless channel data with four body motions: normal gait, abnormal gait (ataxia); and hand reach-out movement with

and without tremors.

- 2) **Classification of motion types:** The next step, we demonstrate that particular features received from wireless channel data generate a unique signature for various types of motions. We examine the data of four various aforementioned body motions and observe that the wireless channel data is unique for each body motion using machine learning algorithm. Based on this narrative, we design a framework that efficiently classifies the four body motions using a machine learning classifier, which trains the acquired data and classifies it with a short period of time.

## II. WIRELESS CHANNEL DATA AND BODY MOTION

Currently, the IEEE 802.11n standards use orthogonal frequency division multiplexing (OFDM) that splits the single carrier channel into several subcarriers and transmits the data into parallel streams [8]. This division of whole frequency spectrum into subcarriers allows OFDM to combat the multipath fading. The wireless channel data obtained using network interface card provides the signal strength raw phase data of OFDM subcarriers. The received signal can be represented as:

$$Y = H \times X + N. \quad (1)$$

Here  $Y$  and  $X$  are the received and transmitted signal, respectively.  $H$  is the channel frequency response (CFR) carrying the wireless channel data and is a complex number that primarily describes the individual subcarrier. The wireless channel data retrieved for all subcarriers can be written as  $l \times m + o$  a matrix, where  $l$  and  $m$  denote the total number of transmitted and received antennas (which is one pair in this study), whereas  $o$  is the total number of subcarriers. The matrix carrying the wireless channel data is fine-grained and accurately records the spectral and temporal conditions of the wireless channel and the changes occurred due to multipath fading. The proposed method uses the fine-grained features of wireless channel data to recognize the abnormal walk and hand tremors when reaching out to grab something, which leads to the detection of cerebellar dysfunction. The wireless channel data is now on a firmware developed by Harperin [9] using network interface card that extracts the wireless channel values in the form of 30 OFDM subcarriers. The equipment used in the proposed method generates particular number of subcarrier. The 30 subcarriers extracted can be expressed as:

$$\mathbf{H} = [H^1, H^2, H^3, \dots, H^{30}]. \quad (2)$$

Here,  $H^i$  denotes the channel frequency response for  $i^{\text{th}}$  subcarrier and is a complex number that describes the signal strength and raw phase data as follows:

$$H^i = \|h\| e^{j\angle\theta}. \quad (3)$$

with  $\|h\|$  the amplitude information and  $\theta$  is the raw wireless channel phase data. It should be noted that the raw channel data obtained using network interface card is extremely random and infeasible for particular motion detection [10]. Thus we calibrate the phase data using linear transformation.

### Wireless Channel Phase Calibration

The variances of amplitude information of wireless channel data have been used in several applications while ignoring the equally important phase information. The aforementioned reason for not leveraging phase data is due to the random noise and unsynchronized clock between the transmitter-receiver pair present in the phase data collected from the network interface card [11]. In this work, the amplitude and phase information are fully leveraged to determine the abnormal walking and hand tremors when reaching out to grab something using linear transformation on raw channel data to remove the random phase offset [12]. Firstly, we consider the measured phase data for  $i^{\text{th}}$  subcarrier.

$$\psi_i' = \psi_i - 2\pi \frac{T_i}{M} \omega + \beta + N. \quad (4)$$

Here  $\psi_i$  denotes the genuine phase,  $\omega$  indicates the time lag,  $T_i$  describes the subcarrier number for  $i^{\text{th}}$  subcarrier ranging from 1 to 30. The terms  $\beta$  and  $M$  represent the phase offset and size of the fast Fourier transform (FFT), respectively. The unknown terms  $\omega$  and  $\beta$  make it impossible to retrieve useful phase information solely from network interface card. To remove the impact of random noise, we employ a linear transformation on the raw wireless channel phase data, as in [13].

### Machine Learning Model for Classifying Body Motion

The amplitude and phase values obtained are classified using machine learning algorithm called support vector machine (SVM). An SVM essentially draws a hyperplane that works as a decision boundary to separate two classes for classification [14]. Suppose we have a problem to classify a dataset in the data-space  $K$  in one of two classes such as  $P$  or  $P'$ . Consider each data point  $k$  is represented by the feature vector  $\vec{k}$  in the feature space  $\bar{X} \subseteq \mathcal{R}^n$ . The given data point  $k\{x_1, x_2, x_3, \dots, x_k\}$  is known as *training data* with the labeled dataset  $\{y_1, y_2, y_3, \dots, y_k\}$ , where  $y_i = 1$ , provided  $x_i \in P$  and  $-1$  otherwise. The goal is to predict new dataset  $k$ , in either one of the two classes. The support vector machine efficiently and accurately resolves this issue [15]. Typically following steps are taken when finite data space is present:

- Firstly a symmetric kernel function is defined,  $Z: X \times X \rightarrow \mathcal{R}$  and the  $k \times k$  matrix  $[K(x_i, x_j)]_{i,j=1}^k$  must be non-negative Eigen values.
- The decision function can be expressed as :

$$F(\alpha) = \sum_{i=1}^k \alpha_i - \frac{1}{2} \sum_{i,j=1}^k y_i y_j \alpha_i \alpha_j K(x_i, x_j). \quad (5)$$

Provided  $\sum_{i=1}^k y_i \alpha_i = 0$  where

$$0 \leq \alpha_i \leq C, i \in (1, k). \quad (6)$$

Considering the  $(\alpha'_1, \alpha'_2, \alpha'_3, \dots, \alpha'_k)$  matrix solution for obtaining the optimum decision boundary. We select  $y_i h_K(x_i) = 1$  for all values of  $i$  when  $0 \leq \alpha'_i < C$ . The training dataset that corresponds to  $(i, \alpha'_i)$  is known as support vectors [16]. The final decision function that classifies the data point  $x$  is  $x \in G$  when  $sign(h_K(x)) = 1$  is written as [17]:

$$h_K(x) = \sum_{i=1 \rightarrow k, x_i \text{ is a support vector}} a'_i y_i | K(x, x_i) + b'. \quad (7)$$

The function represents the hyperplane in  $\bar{X}$  that imparts the training datasets  $X$ . The results obtained using SVM algorithm are presented in terms of percentage accuracy.

### III. EXPERIMENTAL SETTINGS

a). **Experimental environment:** The experiment for detecting cerebellar dysfunction was implemented using small wireless devices, interface card and evaluated the performance in a meeting hall at Xidian University, as shown in Figure 1 and 2.

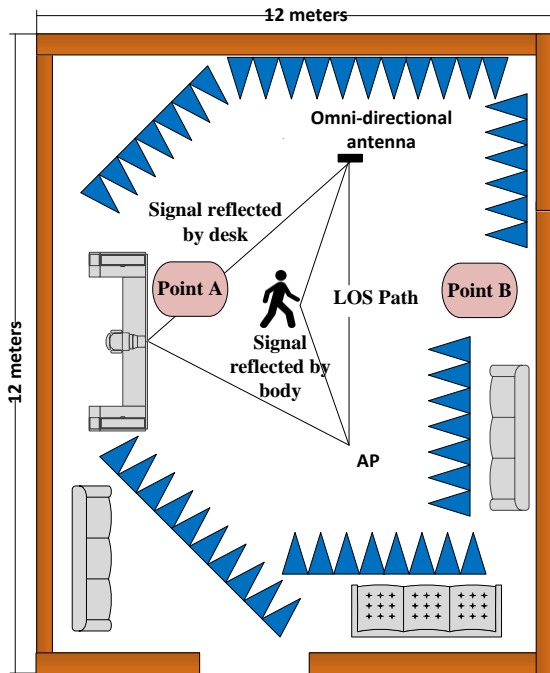


Figure 1 – Experimental setup for identifying gait abnormality

We deployed AD Smart Router operating at S Band as an access point (AP). An HP desktop computer connected to an omnidirectional antenna was used as the receiver. The distance between transmitter and receiver was 8 meters.

The specific type of the absorbing material used in the experiment is FA-500, and the shape is pyramid. The base size is 500\*500mm and the thickness is 500mm.

**b). Experimental Methodology:** A volunteer was asked to walk normally and then walk with abnormality by going back and forth from point A point B as shown in Figure 1. Data is recorded on a desktop computer by pinging the AP to receive the wireless channel packets for measurements.

For the second part of the assessment, the volunteer was asked to grab something with one hand. The router and the receiving antenna placed at 1 meter apart as shown in Figure 2 and the volunteer first grab the glass without tremors in hand and then grabbed it with tremors as experienced by a patient suffering cerebellar dysfunction.

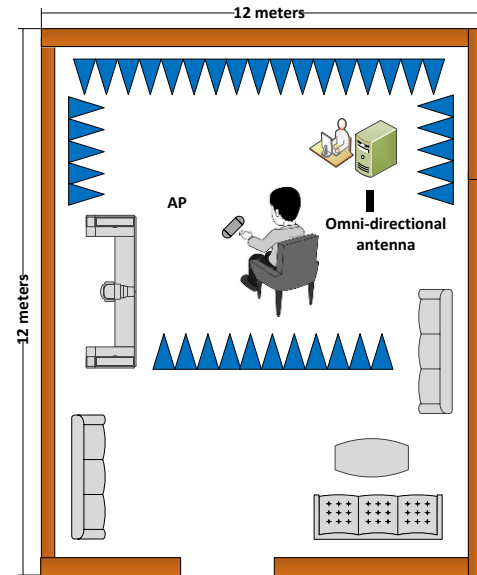


Figure 2 – Volunteer sitting on chair and reaching out to grab something

### IV. IDENTIFYING MOTION USING WIRELESS CHANNEL DATA

This section deals with the effect of certain body motions on wireless channel data. It is observed that body motion changes the multipath of wireless signals propagation, as a result, the individual subcarriers are affected. Each body motion induces a particular wireless channel data. Thus, we demonstrate four various body motions such as normal walk, abnormal walk, normal grab and grabbing with tremors can be differentiated by examining the variances of amplitude information, calibrated phase information retrieved using S-Band sensing technique. In order to extract the wireless channel information features, we first draw statistics in frequency and time domain based on raw wireless channel data. The two extracted set of features are presented in terms of the individual subcarrier and features considering all subcarriers i.e. 30 subcarriers [18].

The features that present the individual subcarrier indicate the variances of amplitude information against a particular subcarrier retrieved using network interface card. The features

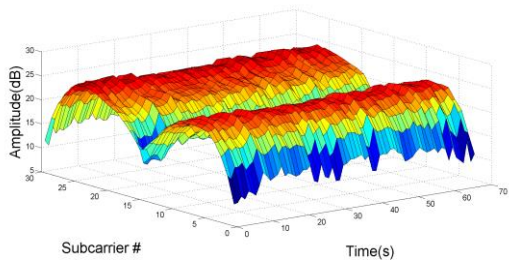
across all subcarriers are calculated by considering the value for a certain wireless channel packet received. Then various statistical wireless channel values are taken for a particular time window considering many wireless channel packets [19]. In addition, to calculate the overall time history of wireless channel information received for a particular time period  $T$  across all subcarriers, we present the following matrix:

$$H_{time\ history} = [\mathbf{H}_1^T, \mathbf{H}_2^T, \mathbf{H}_3^T, \dots, \mathbf{H}_i^T]. \quad (8)$$

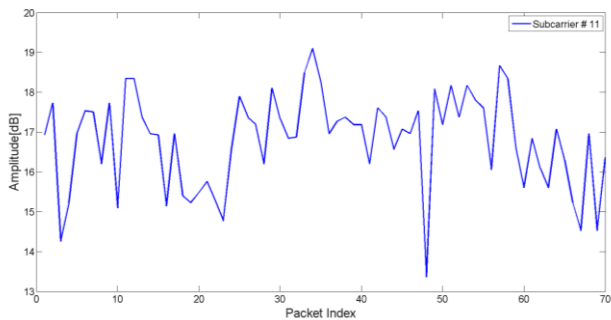
Here  $H_{time\ history}$  denote the overall time history and  $\mathbf{H}_i$  indicate the  $i^{th}$  wireless channel information packet received.

### V. RESULTS AND DISCUSSIONS

The wireless channel data obtained using network interface card when the host computer was connected to the AP to detect the two primary indicators: to record the tremors in hand while reaching out to grab something and ataxia.



(a). Raw wireless channel data: variances of the amplitude of 30 subcarriers for 70 seconds.



(b). Variances of the individual subcarrier for 70 seconds.

Figure 3 – The wireless channel data retrieved when subject was reaching out to grab something without tremor in hand

The goal of analyzing the variances of amplitude and calibrated phase information is to differentiate the hand movements with and without tremors when reaching out to grab something. Figure 3(a) shows the variances of raw amplitude data for 30 subcarriers over a period of 70 seconds. The main advantage of this S-Band sensing technique is that we can choose any one or multiple subcarriers against time history for analysis. In order to differentiate the tremors and non-tremors in hand, we examine subcarrier # 11 in Figure 3(b), which indicate the variances in amplitude information between 14 dB and 17 dB. We further examined the calibrated phase

information after applying the linear transformation on raw wireless phase data as shown in Figure 4.

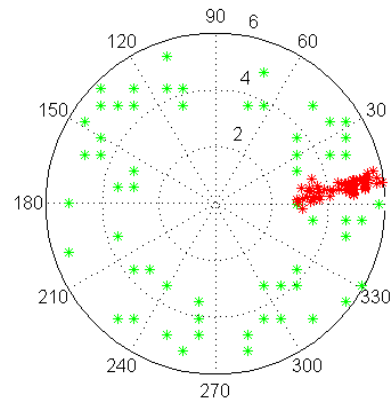
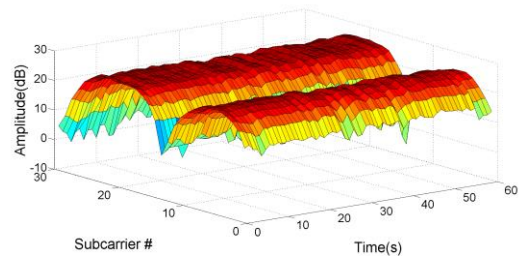
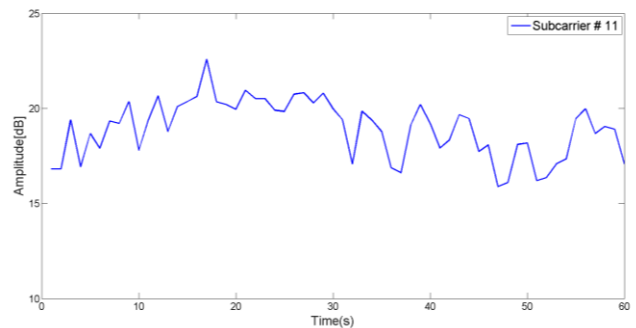


Figure 4 – Calibrated phase information for grabbing something without tremor in hand

In order to analyze the second primary indicator for detecting the cerebellar dysfunction, we study the calibrated phase information as in Figure 4. The data in green indicate the raw phase data and the phase information in red denote the calibrated phase information. The calibrated phase information recorded when the subject was reaching out for grabbing something is plotted between  $0^0$  and  $10^0$  from 4 dB to 6 dB. The amplitude and calibrated phase information that are recorded for person grabbing something with tremors are observed in Figure 5 and 6, respectively.



(a). Variances of the amplitude of 30 subcarriers for 60 seconds.



(b). The amplitude information of 11<sup>th</sup> subcarrier for 60 seconds.

Figure 5 – The wireless channel data recorded when subject was repeated grabbing something with tremors in hand

Figure 5(a) shows the variation of amplitude information when the subject reaches out to grab something repeatedly. The data, in this case, is collected for 60 seconds. Figure 5(b)

describes the amplitude information of the 11<sup>th</sup> subcarrier when the subject grabbed something with a tremor, which varied between 14 dB and 23 dB.

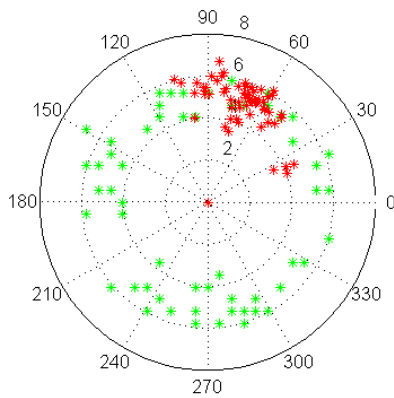


Figure 6 – Calibrated phase information for reaching out to grab something with tremors in hand

The calibrated phase information for grabbing something within tremors in hands in Figure 6 is mostly plotted between 50<sup>o</sup> and 100<sup>o</sup>. When this calibrated phase information is compared with Figure 4, we observe that each movement such as tremor in hands and non-tremors in hands generated a unique pattern which clearly distinguishes the two motions for detecting cerebellar dysfunction. In order to observe the time history of the two body motions, we examine the Figure 7.

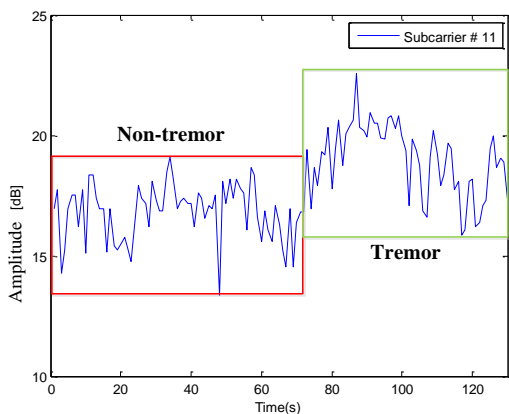


Figure 7 – Time history of two motions such as non-tremors and tremors in hands

The time history of 11<sup>th</sup> subcarrier presenting non-tremors and tremors when the subject was reaching out to grab something for a period of 130 seconds is shown in Figure 7. From 0 to the 70<sup>th</sup> second, the variances of amplitude information indicated no tremors, whereas from the 70<sup>th</sup> second to the 130<sup>th</sup> second, the variations described the tremors in hands. We observe that the power level for each motion is different but there are moments with similarity in the power level in dB. For example, from the 20<sup>th</sup> second to the 40<sup>th</sup> second and the 110<sup>th</sup> second to the 120<sup>th</sup> second, the power levels are almost the same that make it difficult the differentiate the two motions using the time history. Thus we classify the data obtained using S-Band sensing technique using support vector machine.

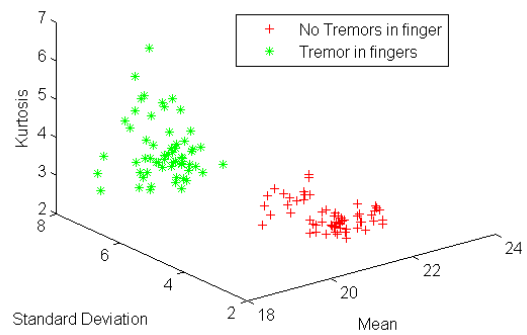


Figure 8 - Two motion represented in their feature space

The first goal to classify the data retrieved using S-Band sensing technique was to identify the particular features that would play the role of a fingerprint of the wireless channel traces. Initially, a limited number of possible features were defined, from which the best performers were selected as shown in Figure 8. The best possible features such as *mean*, *standard deviation* and *kurtosis* were considered for classification using SVM algorithm.

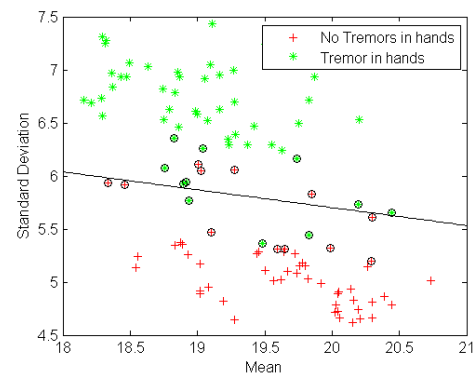
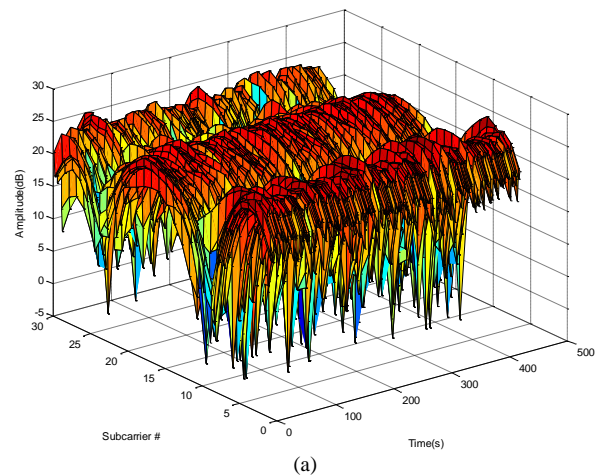
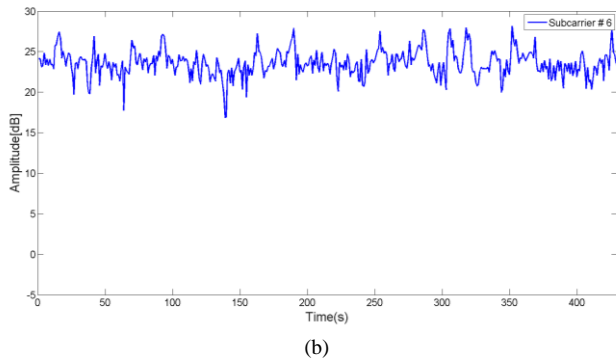


Figure 9 – The SVM results obtained considering mean and standard deviation

The SVM algorithm obtained an accuracy of 91% when the two features such as mean and standard deviation were considered for classifying the non-tremors and tremors in hands.





(a). Perturbations of amplitude information of 30 subcarriers for 450 seconds.  
 (b). Variances of amplitude information for individual subcarrier.  
 Figure 10 – The wireless channel information obtained when subject was walking normally around the room

To examine the second primary indicator for detecting cerebellar dysfunction, we consider the data obtained in Figure 10. The variations in amplitude information against 30 subcarriers for 450 seconds are shown in Figure 10(a) and the perturbations of amplitude information that fluctuate between 18 dB and 26 dB for 450 seconds is illustrated in Figure 10(b). Next, we discuss the calibrated phase information in Figure 11 for a person’s normal walk around the room.

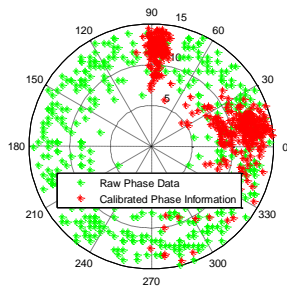
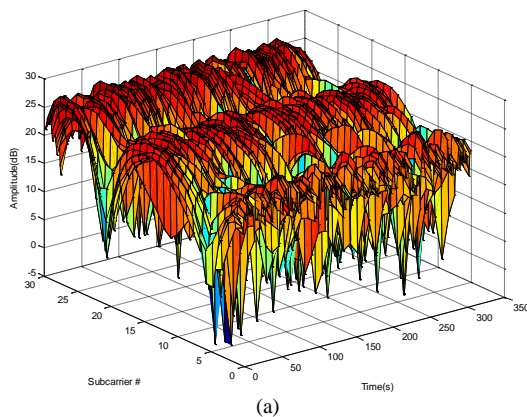
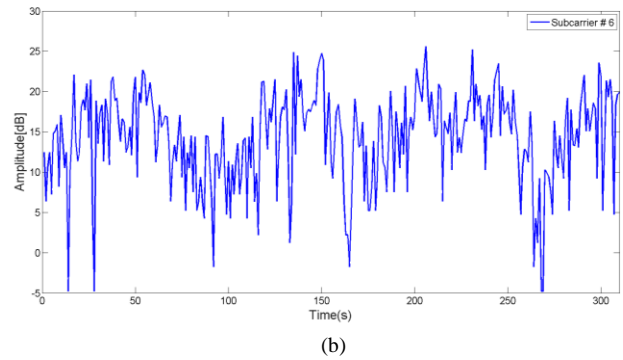


Figure 11 – Calibrated phase information when subject was walking in indoor environment

As far as the calibrated phase information is concerned when the normal walk was considered, we have obtained two clusters of data that is spread from  $30^{\circ}$  to  $270^{\circ}$  and  $85^{\circ}$  to  $90^{\circ}$ . The reason for dispersed phase information is due to the fact person walks around the room. As a result, there is continuous change in the wireless medium.



(a)



(b)

Figure 12 – The wireless channel information obtained when subject was walking abnormally around the room

Figure 12(a) indicates the raw wireless channel data when the person was walking abnormally around the room, and Figure 12(b) describes the time history of individual subcarrier 330 seconds. The amplitude information, in this case, fluctuates between -5 dB and 25 dB.

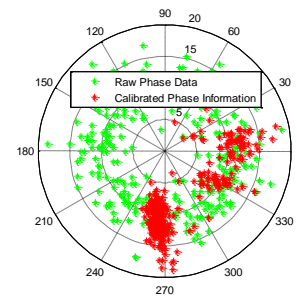


Figure 13 – Calibrated phase information when person was walking in an abnormal manner (ataxia)

The calibrated phase information extracted using S-Band sensing technique is scattered from  $30^{\circ}$  to  $250^{\circ}$  that fluctuate between 5 dB to 20 dB. We further combine the individual subcarrier (6<sup>th</sup> in this case) to examine the overall time history of a person walking normally and undergoing ataxia attacks.

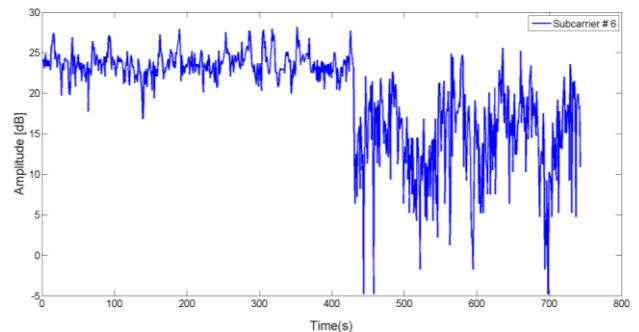


Figure 14 – Overall time history of person performing walking activity

The overall time history of 6<sup>th</sup> subcarrier shows a clear sign of a shift in power level when was first started walking normally from 0 to 450<sup>th</sup> second and then experienced ataxia attack (abnormal walk) from 450<sup>th</sup> second till the 780<sup>th</sup> second. The power level in the case of the former varies between 18 dB and 26 dB, whereas in the latter case, it fluctuates between -5 dB and 25 dB as indicated in Figure 14. It should be noted that

the power level will be different when the system is deployed in different geometrical structure. We can see in both cases when the person was reaching out to grab something and in walking activity, each body motion has induced a unique an imprint that can be leveraged to identify a particular disease such as cerebellar dysfunction. The idea of analyzing the individual subcarrier is to see the time when the patient has observed a particular abnormal motion such as tremors in hands or abnormal walk. To determine the accuracy in terms of percentage of the data obtained for a *normal walk* and *abnormal walk*, we consider the 30 subcarriers data and classify it using SVM as indicated in Figure 15.

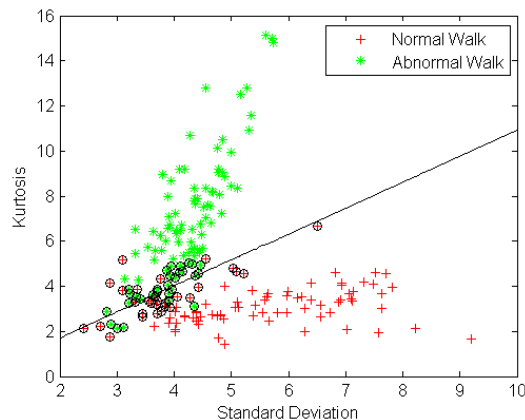


Figure 15 – The SVM results obtained for classifying normal and abnormal walk

The SVM results obtained by considering the standard deviation and kurtosis as the two features for classification as shown in Figure 15. The results show an accuracy of 93% when the 30 subcarrier data was considered. A different kernel function was used since the data was recorded as different experimental setup was made.

## VI. CONCLUSION

A framework which can easily be deployed in the clinical settings was developed by evaluating the two abnormal body motions, gait abnormality and tremors in hand. This framework uses S-Band sensing technique that leveraged low-cost small wireless devices, which provided seamless data reception. The proposed framework utilized the variances of amplitude and calibrated phase information that induced a unique wireless channel imprint to identify the particular motion disorders. The data classification was performed using support vector machine that provided high classification accuracy.

## VII. ACKNOWLEDGEMENT

The authors would like to thank Northwest Women's and Children's Hospital for their help and guidance during the experiments.

## VIII. CONCLUSION

[1]. A. Geminiani, A. Pedrocchi, E. D'Angelo and C. Casellato, "Spiking cerebellar model with damaged cortical Neural population reproduces human ataxic behaviors in perturbed upper limb reaching," *2017 8th International*

*IEEE/EMBS Conference on Neural Engineering (NER)*, Shanghai, 2017, pp. 489-492.

[2]. Ann-Kathrin Seifert, Abdelhak M. Zoubir, Moeness G. Amin, "Radar Classification of Human Gait Abnormality Based on Sum-of-Harmonics Analysis," *2018 IEEE Radar Conference (RadarConf18)*, pp. 940-945, 2018.

[3]. Chester Rei E. Duhaylungsod, Czarina Eloise B. Magbitang, Jan Faith Isaac R. Mercado, George Elison D. Osido, Shannen Andrea C. Pecho, Angelo R. dela Cruz, "Detection of Gait Abnormality through Leg Symmetry and Temporal Parameters," *2017 IEEE 9th International Conference on Humanoid, Nanotechnology, Information Technology, Communication and Control, Environment and Management (HNICEM)*, pp. 1-4, 2017.

[4]. Ada Zhang, Alexander Cebulla, Stanislav Panev, Jessica Hodgins, "Weakly-supervised Learning for Parkinson's Disease Tremor Detection," *2017 39th Annual International Conference of the IEEE Engineering in Medicine and Biology Society (EMBC)*, pp. 143-147, 2017.

[5]. Abbas Ismail, Hassan Shouman, Ali Cherry, Mohamad Hajj-Hassan, "Towards Real Time Kinect Analysis System for Early Diagnosis of Gait Cycle Abnormalities," *2017 Fourth International Conference on Advances in Biomedical Engineering (ICABME)*, pp. 1-4, 2017.

[6]. Mehmet Akif Alper, Daniel Morris, Luan Tran, "Remote Detection and Measurement of Limb Tremors," *2018 5th International Conference on Electrical and Electronic Engineering (ICEEE)*, pp. 198-202, 2018.

[7]. Mingmin Zhao, Shichao Yue, Dina Katabi, Tommi S. Jaakkola, Matt T. Bianchi, "Learning Sleep Stages from Radio Signals: A Conditional Adversarial Architecture," *Proceedings of the 34th International Conference on Machine Learning*, pp. 4100-4109, 2017.

[8]. W. Cao, X. Li, W. Hu, J. Lei and W. Zhang, "OFDM reference signal reconstruction exploiting subcarrier-grouping-based multi-level Lloyd-Max algorithm in passive radar systems," in *IET Radar, Sonar & Navigation*, vol. 11, no. 5, pp. 873-879, 5 2017.

[9]. D. Halperin, W. Hu, A. Sheth, and D. Wetherall. "Tool release: Gathering 802.11n traces with channel state information." *ACM SIGCOMM CCR*, 41(1):53, Jan. 2011

[10]. J. Xiao, K. Wu, Y. Yi, L. Wang, and L. M. Ni, "Pilot: Passive device-free indoor localization using channel state information," in *Proc. 33rd Int. Conf. IEEE Distrib. Comput. Syst.*, 2013, pp. 236-245.

[11]. J. Xiao, K. Wu, Y. Yi, L. Wang, and L. M. Ni, "Pilot: Passive device-free indoor localization using channel state information," in *Proceedings of IEEE ICDCS. IEEE*, 2013, pp. 236-245. M. Young, *The Technical Writers Handbook*. Mill Valley, CA: University Science, 1989.

[12]. K. Qian, C. Wu, Z. Yang, Y. Liu and Z. Zhou, "PADS: Passive detection of moving targets with dynamic speed using PHY layer information," *2014 20th IEEE International Conference on Parallel and Distributed Systems (ICPADS)*, Hsinchu, 2014, pp. 1-8.

[13]. K. Qian, C. Wu, Z. Yang, Y. Liu and Z. Zhou, "PADS: Passive detection of moving targets with dynamic speed using PHY layer information," *2014 20th IEEE International Conference on Parallel and Distributed Systems (ICPADS)*, Hsinchu, 2014, pp. 1-8.

[14]. W. Wang, J. Xi, A. Chong and L. Li, "Driving Style Classification Using a Semisupervised Support Vector Machine," in *IEEE Transactions on Human-Machine Systems*, vol. 47, no. 5, pp. 650-660, Oct. 2017.

[15]. V.N. Vapnik, *Statistical Learning Theory*. Wiley-Interscience, 1998.

[16]. E. Ergul, N. Arica, N. Ahuja and S. Erturk, "Clustering Through Hybrid Network Architecture With Support Vectors," in *IEEE Transactions on Neural Networks and Learning Systems*, vol. 28, no. 6, pp. 1373-1385, June 2017.

[17]. X. Pan, H. Yang, L. Li, Z. Liu and L. Hou, "FPGA Implementation of SVM Decision Function Based on Hardware-Friendly Kernel," *2013 International Conference on Computational and Information Sciences*, Shiyang, 2013, pp. 133-136.

[18]. S. A. Shah *et al.*, "Posture Recognition to Prevent Bedsores for Multiple Patients Using Leaking Coaxial Cable," in *IEEE Access*, vol. 4, pp. 8065-8072, 2016.

[19]. X. Liu, J. Cao, S. Tang, J. Wen and P. Guo, "Contactless Respiration Monitoring Via Off-the-Shelf WiFi Devices," in *IEEE Transactions on Mobile Computing*, vol. 15, no. 10, pp. 2466-2479, Oct. 1 2016.